

TRANSVERSE BEAM EMITTANCE MEASUREMENTS OF A 16 MeV LINAC AT THE IDAHO ACCELERATOR CENTER

S. Setiniyaz*, K. Chouffani, T. Forest, and Y. Kim
 Idaho State University, Pocatello, ID, 83209, USA
 A. Freyberger, Jefferson Lab, Newport News, Virginia, 23606, USA

Abstract

A beam emittance measurement of a 16 MeV S-band High Repetition Rate Linac (HRRL) was performed at Idaho State University's Idaho Accelerator Center (IAC). The HRRL linac structure was upgraded beyond the capabilities of a typical medical linac so it can achieve a repetition rate of 1 kHz. Measurements of the HRRL transverse beam emittance are underway that will be used to optimize the production of positrons using HRRL's intense electron beam on a tungsten converter. In this paper, we describe a beam imaging system using an OTR screen and a digital CCD camera, a MATLAB tool to extract beam size and emittance, detailed measurement procedures, and the results of measured transverse emittances for an arbitrary beam energy.

INTRODUCTION

The HRRL is an S-band electron linac located in the beam lab of the Physics Department at Idaho State University (ISU). The HRRL accelerates electrons to energies between 3 and 16 MeV with a maximum repetition rate of 1 kHz. The HRRL beamline has recently been reconfigured to generate and collect positrons.

An Optical Transition Radiation (OTR) based viewer was installed to allow measurements at the high electron currents available using the HRRL. The visible light from the OTR based viewer is produced when a relativistic electron beam crosses the boundary of two mediums with different dielectric constants. When the electron beam intersects the OTR target at a 45° angle, visible radiation is emitted at an angle of 90° with respect to the incident beam direction [1]. These backward-emitted photons are observed using a digital camera and can be used to measure the shape and intensity of the beam based on the OTR image distribution.

Emittance is a key parameter in accelerator physics that is used to quantify the quality of an electron beam produced by an accelerator. An emittance measurement can be performed in a several ways [2, 3]. This work used the Quadrupole scanning method [4] to measure emittance, Twiss parameters, and the beam energy.

THE EXPERIMENT

Quadrupole Scanning Method

As shown in Fig. 1 illustrates the basic components used to measure the emittance with the quadrupole scanning method. A quadrupole is positioned at the exit of the linac to focus or de-focus the beam as observed on a downstream view screen. The distance between the quadrupole and the screen was chosen in order to minimize chromatic effects and to satisfy the thin lens approximation. Assuming the

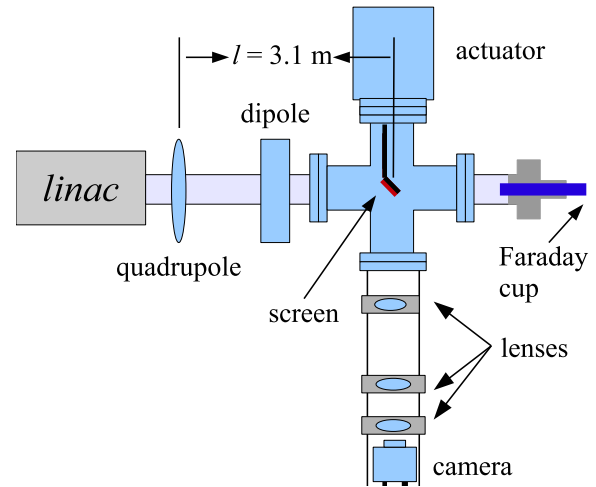


Figure 1: Apparatus used to measure the beam emittance.

thin lens approximation, $\sqrt{k_1}L \ll 1$, is satisfied, the transfer matrix of a quadrupole magnet may be expressed as

$$\mathbf{Q} = \begin{pmatrix} 1 & 0 \\ -k_1 L & 1 \end{pmatrix} = \begin{pmatrix} 1 & 0 \\ -\frac{1}{f} & 1 \end{pmatrix}, \quad (1)$$

where k_1 is the quadrupole strength, L is the length of quadrupole, and f is the focal length. A matrix representing the drift space between quadrupole and screen is given by

$$\mathbf{S} = \begin{pmatrix} 1 & l \\ 0 & 1 \end{pmatrix}, \quad (2)$$

where l is the distance between the scanning quadrupole and the screen. The transfer matrix of the scanning region is given by the matrix product $\mathbf{M}\mathbf{Q}$. In the horizontal plane, the beam matrix at the screen (σ_s) is related to the beam matrix of the quadrupole (σ_q) using the similarity transformation

$$\sigma_s = \mathbf{M}\sigma_q\mathbf{M}^T. \quad (3)$$

* Email: sadik82@gmail.com

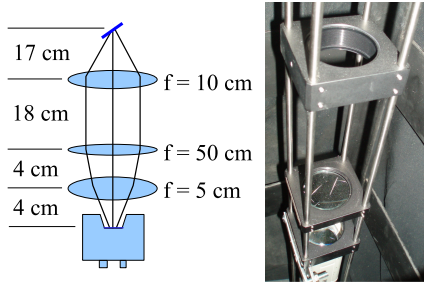


Figure 2: The OTR Imaging system.

where the σ_s and σ_q are defined as [5]

$$\sigma_{s,x} = \begin{pmatrix} \sigma_{s,x}^2 & \sigma_{s,xx'} \\ \sigma_{s,xx'} & \sigma_{s,x'}^2 \end{pmatrix}, \quad \sigma_{q,x} = \begin{pmatrix} \sigma_{q,x}^2 & \sigma_{q,xx'} \\ \sigma_{q,xx'} & \sigma_{q,x'}^2 \end{pmatrix}. \quad (4)$$

By defining the new parameters [4]

$$A \equiv l^2 \sigma_{q,x}^2, \quad B \equiv \frac{1}{l} + \frac{\sigma_{q,xx'}}{\sigma_{q,x}^2}, \quad C \equiv l^2 \frac{\epsilon_x^2}{\sigma_{q,x}^2}. \quad (5)$$

the matrix element describes the square of the rms beam size at the screen, $\sigma_{s,x}^2$, becomes a parabolic function of the product of k_1 and L

$$\sigma_{s,x}^2 = A(k_1 L)^2 - 2AB(k_1 L) + (C + AB^2). \quad (6)$$

The emittance measurement was performed by changing the quadrupole current, which changes $k_1 L$, and measuring the corresponding beam image on the view screen. The measured two-dimensional beam image was projected along the images abscissa and ordinate axes. A Gaussian fitting function is used on each projection to determine the rms value, σ_s in Eq. (6), of the image along each axis. Measurements of σ_s for several quadrupole current ($k_1 L$) is then fit using the parabolic function in Eq. (6) to determine the constants A , B , and C . The emittance (ϵ) and the Twiss parameters (α and β) can be found using Eq. (7).

$$\epsilon = \frac{\sqrt{AC}}{l^2}, \quad \beta = \sqrt{\frac{A}{C}}, \quad \alpha = \sqrt{\frac{A}{C}} \left(B + \frac{1}{l} \right). \quad (7)$$

The OTR Imaging System

The OTR target is 10 μm thick aluminum foil with a 1.25 inch of diameter. The OTR is emitted in a cone shape with the maximum intensity at an angle $1/\gamma$ with respect to the reflecting angle of the electron beam [1]. Three lenses, 2 inches in diameter, are used for the imaging system to avoid optical distortion at lower electron energies. Focal lengths and position of the lenses are shown in Fig. 2. The camera used was a JAI CV-A10GE digital camera with 767 by 576 pixel area. The camera images were taken by triggering the camera during synchronously with the electron gun.

Quadrupole Scanning

The current for one of the beam line quadrupoles is changed to alter the strength and direction of the

quadrupole magnetic field such that a measurable change in the beam shape is seen by the OTR system. Initially, the beam was steered by the quadrupole indicating that the beam was not entering along the quadrupoles central axis. Several magnetic elements upstream of this quadrupole were adjusted to align the incident electron beam with the quadrupoles central axis. First, the beam current observed by a Faraday cup located at the end of beam line was maximized using upstream steering coils within the linac nearest the gun. Second, the first solenoid nearest the linac gun was used to focus the electron beam on the OTR screen. Steering coils were adjusted to maximum the beam current to the FC and minimize the deflection of the beam by the solenoid first then by the quadrupole. A second solenoid and the last steering magnet, both near the exit of the linac, were used in the final step to optimize the beam spot size on the OTR target and maximize the Faraday cup current. A configuration was found that minimized the electron beam deflection when the quadrupole current was altered during the emittance measurements.

The emittance measurement was performed using an electron beam energy of 15 MeV and a 40 mA macro pulse peak current. The current in the first quadrupole after the exit of the linac was changed from -5 A to 5 A with an increment of 0.2 A. Seven measurements were taken at each current step in order to determine the average beam width and the variance. Background measurements were taken by turning the linac's electron gun off while keep the RF on. Background image and beam images before and after background subtraction are shown in Fig. 3. A small dark current is visible in Fig. 3b that is known to be generated when electrons are pulled off the cavity wall and accelerated.

The electron beam energy was measured using a dipole magnet downstream of the quadrupole used for the emittance measurements. Prior to energizing the dipole, the electron micro-pulse bunch charge passing through the dipole was measured using a Faraday cup located approximately 50 cm downstream. The dipole current was adjusted until a maximum beam current was observed on another Faraday cup located just after the 45 degree exit port of the dipole. A magnetic field map of the dipole suggests that the electron beam energy was 15 MeV. Future emittance measurements are planned to cover the entire energy range of the linac.

Data Analysis and Results

Images from the JAI camera were calibrated using the OTR target frame. An LED was used to illuminate the OTR aluminum frame that has a known inner diameter of 31.75 mm. Image processing software was used to inscribe a circle on the image to measure the circular OTR inner frame in units of pixels. The scaling factor can be obtained by dividing this length with the number of pixels observed. The result is a horizontal scaling factor is 0.04327 ± 0.00016 mm/pixel and vertical scaling factor is 0.04204 ± 0.00018 mm/pixel. Digital images from the JAI

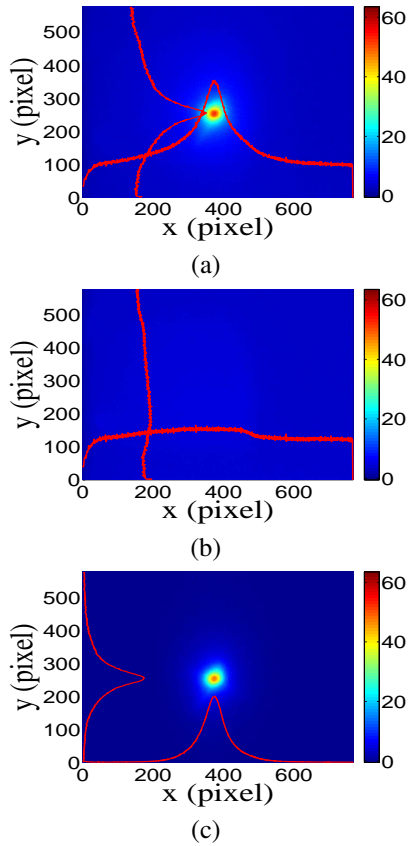


Figure 3: Background subtracted to minimize impact of dark current; (a) a beam with the dark current and background noise, (b) a background image, (c) a beam image when dark background was subtracted.

camera were extracted in a matrix format in order to take projections on both axes and perform a Gaussian fit. The observed image profiles were not well described by a single Gaussian distribution. The profiles may be described using a Lorentzian distribution, however, the rms of the Lorentzian function is not defined. The super Gaussian distribution seems to be the best option [6], because rms values may be directly extracted.

Fig. 4 shows the square of the rms (σ_s^2) vs k_1L for x (horizontal) and y (vertical) beam projections along with the parabolic fits using Eq. 6. The emittances and Twiss parameters from these fits are summarized in Table. 1. Further details describing the fitting procedures are described in reference [7]. The normalized emittance obtained by projected emittance multiplied with average relativistic factor γ and β of the electron beam.

CONCLUSIONS

A diagnostic tool was developed and used to measure the beam emittance of the High Rep Rate Linac at the Idaho Accelerator Center. The tool relied on measuring the images generated by the optical transition radiation of the electron beam on a polished thin aluminum target. The

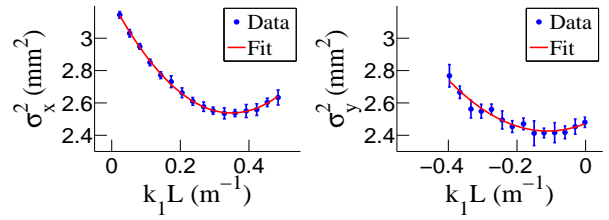


Figure 4: Square of rms values and parabolic fittings.

Table 1: Emittance Measurement Results.

Parameter	Unit	Value
projected emittance ϵ_x	μm	0.37 ± 0.02
projected emittance ϵ_y	μm	0.30 ± 0.04
normalized emittance $\epsilon_{n,x}$	μm	10.10 ± 0.51
normalized emittance $\epsilon_{n,y}$	μm	8.06 ± 1.1
β_x -function	m	1.40 ± 0.06
β_y -function	m	1.17 ± 0.13
α_x -function	rad	0.97 ± 0.06
α_y -function	rad	0.24 ± 0.07
micro-pulse charge	pC	11
micro-pulse length	ps	350.16
energy of the beam E	MeV	15
relative energy spread $\Delta E/E$	%	10.4

electron beam profile was not described well using a single Gaussian distribution but rather a super Gaussian or Lorentzian distribution. The system appears to more accurately measure the beam's horizontal size because of the larger dynamic range of the imaging system's pixels. The normalized emittance of the High Rep Rate Linac, similar to medical linacs, at ISU was measured to be less than $10 \mu\text{m}$ when accelerating electrons to an energy of 15 MeV as measured by the OTR based tool described above.

ACKNOWLEDGMENT

We would like to acknowledge the outstanding efforts of Idaho Accelerator Center. This work was supported by DOE award # DE-SC0002600.

REFERENCES

- [1] B. Gitter, Tech. Rep., Los Angeles, USA (1992).
- [2] K.T. McDonald and D.P. Russell, Fron. of Par. Beams Obser. Diag. and Cor. **08544**, (1988).
- [3] Y. Kim *et al.*, in *Proc. FEL2008*, Gyeongju, Korea.
- [4] D.F.G. Benedetti, *et al.*, Tech. Rep., DAFNE Tech. Not., Frascati, Italy (2005).
- [5] S.Y. Lee, *Accelerator Physics*, (Singapore: World Scientific, 2004), 61.
- [6] F.J. Decker, NASA STI/Recon Tech. Rep. N **1996**, (1994) 10487.
- [7] C.F. Eckman *et al.*, in *Proc. IPAC2012*, New Orleans, USA.